CIRCULATORY STREAMING AROUND AN OSCILLATING ELLIPTIC CYLINDER

TATSUNO, Masakazu
Research Institute for Applied Mechanics, Kyushu University: Research Associate

https://doi.org/10.5109/7173445

出版情報：Reports of Research Institute for Applied Mechanics. 22 (71), pp.313-325, 1975. 九州大学応用力学研究所

Reports of Research Institute for Applied Mechanics
Vol. XXII, No. 71, 1975

CIRCULATORY STREAMING AROUND AN OSCILLATING ELLIPTIC CYLINDER*

By Masakazu TATSUNO**

The secondary flow generated by an oscillating elliptic cylinder was investigated experimentally. The elliptic cylinder was oscillated sinusoidally in a fluid enclosed by a circular cylindrical container. When the minor axis of the elliptic cylinder is inclined at an angle 45° with the axis of oscillation, the flow pattern of the circulatory streaming has symmetry with respect to a turn of 180 degrees around the center axis of the cylinder. The distance between the cores of the inner vortex systems and the center axis of the cylinder is large at small values of $r_0\sqrt{\omega/\nu}$, and becomes smaller with increasing the values of $r_0\sqrt{\omega/\nu}$, where r_0 is the representative length of the elliptic cylinder, ω the angular frequency and ν the kinematic viscosity. The position of stagnation points on the cylinder surface is independent of both the values of $r_0\sqrt{\omega/\nu}$ and s/r_0, where s is the oscillation amplitude.

1 Introduction

It is well known that when a bluff body is oscillated sinusoidally in a fluid, the secondary flow is generated around the body due to the nonlinear effect of the fluid flow. The flow field around the body is generally divided into two main regions, that is, the inner boundary layer and the outer flow region. The inner boundary layer consists of the inner vortex systems and the outer flow region the outer vortex systems.

Many investigations of the streaming around a circular cylinder [1-10] or a sphere [11-14] have been done both theoretically and experimentally, and Tatsuno investigated the streaming around a regular square cylinder [15] experimentally. On the basis of these investigations, the flow patterns of the streaming around these bodies are symmetric with respect to both the axis of oscillation and the axis perpendicular to it.

Moreover, Tatsuno investigated the streaming around an oscillating triangular cylinder [16]. When the triangular cylinder is oscillated perpendicularly to one of its sides, the flow pattern around the cylinder is symmetric with respect to the axis of oscillation but asymmetric with respect to the axis perpendicular to it. On the other hand, when the triangular cylinder is oscillated parallel with one of its sides, the flow pattern is asymmetric with

*This work was read at the Annual Meeting of the Physical Society of Japan held in Chiba (October 12, 1974)

**Research Associate, Research Institute for Applied Mechanics, Kyushu University

respect to the axis of oscillation but symmetric with respect to the axis perpendicular to it. In this way, if the body is symmetric with respect to either the axis of oscillation or the axis perpendicular to it, the flow pattern of the streaming is symmetric with respect to the same axis.

The purpose of this work is to investigate the flow pattern of the streaming around a body asymmetric with respect to both the axis of oscillation and the axis perpendicular to it. In this work, an elliptic cylinder was used as a test body. It is symmetric with respect to its own two axes, the major one and the minor. When the minor axis, however, is inclined at an angle 45° with the axis of oscillation, the cylinder is asymmetric with respect to both the axis of oscillation and the axis perpendicular to it.

2 Apparatus and Experimental Method

The experiments were carried out with the same apparatus that the author used in the previous experiments on the streaming around oscillating circular cylinders, square cylinders or triangular cylinders. Figure 1 shows the essential elements of the apparatus used in this work. A loudspeaker was used to oscillate an elliptic cylinder. Oscillating motion of the loudspeaker cone was communicated to the cylinder through a support rod attached to the cone. The size of the elliptic cylinder made of wood was 0.558 cm in major axis, 0.374 cm in minor axis, 0.742 in eccentricity and 6.0 cm in length for the case of the minor axis inclining at an angle 45° with the axis of oscillation. On the other hand, the size of it was 0.546 cm in major axis, 0.358 cm in minor axis, 0.755 in eccentricity and 6.0 cm in length for the case of the minor axis coinciding with the axis of oscillation. The representative length of the cylinder section is defined as $r_0 \equiv \sqrt{a^2-b^2}$, where a is half the length of the major axis and b half the length of the minor axis. The fluid was a mixture of water and glycerin, and the kinematic viscosity ranged from 0.087 cm^2/s to 2.03 cm^2/s. The size of a circular cylindrical container of the fluid was 6.1 cm in radius and 5.5 cm in depth. The value of R_0/r_0 is 29.5 and 29.6 respectively for two cases, where R_0 is the radius of the container. Under these conditions, on the basis of past

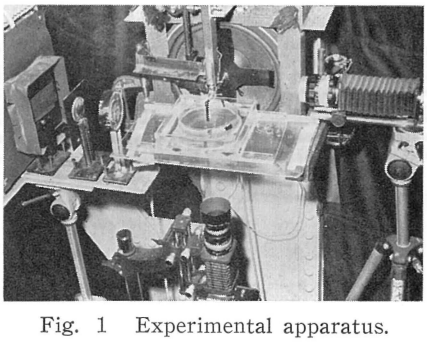

Fig. 1 Experimental apparatus.

works, the inner vortex systems in the vicinity of the cylinder can be expected to be irrespective of the shape and the size of the container. The axis of the container coincided with that of the cylinder at rest. Underneath the container a camera was placed to take photographs of the motion of aluminium dust or glass micro-particles which were suspended uniformly in the fluid. A stroboscope was used for illuminating a plane perpendicular to the axis of the cylinder.

3 Experimental Results

3-1 Case of the minor axis inclining at an angle 45° with the axis of oscillation

The flow pattern in the vicinity of the cylinder is generally considered

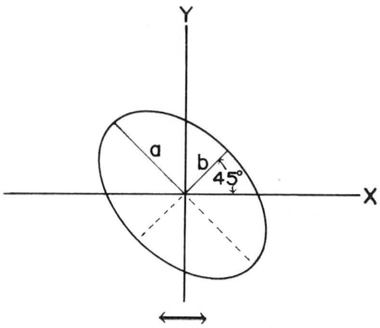

Fig. 2 Configuration of the elliptic cylinder.

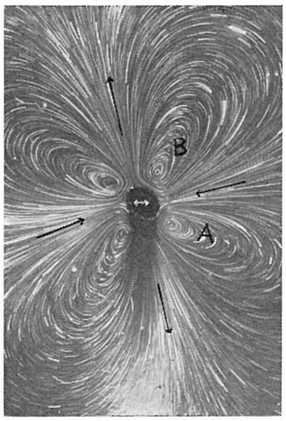

Fig. 3 Inner vortex systems photographed in stroboscopic light, synchronized with the oscillation of an elliptic cylinder. $r_0=0.207$ cm, $f=\omega/2\pi=30.1$ Hz, $s=0.0282$ cm, $\nu=2.03$ cm^2/s, $r_0\sqrt{\omega/\nu}=2.00$, $s/r_0=0.136$, Exposure time $t_e=60$ s.

Aluminium dust and glass micro-particles were added to serve as tracers.

to be characterized by r_0, ω, s and ν, where ω is the angular frequency, s the oscillation amplitude and ν the kinematic viscosity. Therefore, we have two independent non-dimensional parameters $r_0\sqrt{\omega/\nu}$ and s/r_0. The configuration of the elliptic cylinder is shown in Fig. 2. The double arrow in this figure indicates the direction of oscillation.

The photograph in Fig. 3 shows the streaming around an elliptic cylinder at $r_0\sqrt{\omega/\nu}=2.00$. The arrow indicates the direction of the flow. As will

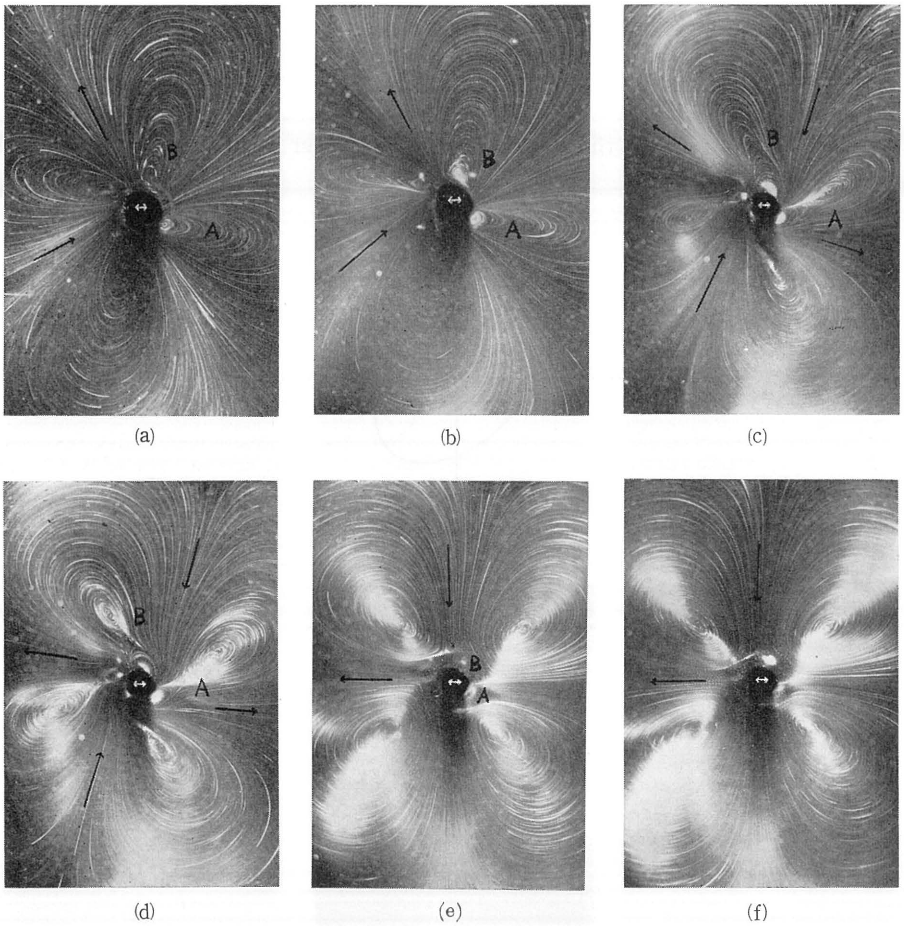

Fig. 4 Consecutive stages of the flow around an elliptic cylinder when the oscillation amplitude was increased in steps.
$r_0=0.207$ cm, $f=50.1$ Hz, $\nu=0.81$ cm^2/s, $r_0\sqrt{\omega/\nu}=4.08$.
(a) $s/r_0=0.150$, $t_e=60$ s (b) $s/r_0=0.376$, $t_e=60$ s
(c) $s/r_0=0.768$, $t_e=15$ s (d) $s/r_0=0.821$, $t_e=15$ s
(e) $s/r_0=1.01$, $t_e=10$ s (f) $s/r_0=1.16$, $t_e=10$ s
Aluminium dust and glass micro-particles were added to serve as tracers.

be seen from this figure, the inner boundary layer next to the cylinder consists of four inner vortex systems, with a direction of circulation such that the flow is toward the cylinder at a small angle with the axis of oscillation. In this case, as the value of $r_0\sqrt{\omega/\nu}$ is small, the inner vortex systems extend broadly. The vortex systems (A) and (B) have the reversed flow direction each other, where the symbols (A) and (B) are written in the figure. The flow pattern has symmetry with respect to a turn of 180 degrees around the center axis of the cylinder.

Some photographs in Fig. 4 show the consecutive stages of the flow around the cylinder when the oscillation amplitude was increased in steps at $r_0\sqrt{\omega/\nu}=4.08$. The inner vortex systems extend broadly at small values of oscillation amplitude, as shown in Fig. 4 (a) and (b). When the oscillation amplitude is increased more, as will be seen from Fig. 4 (c), the inner vortex system (A) divides into two systems with the same flow direction, the very small one beside the cylinder and the larger one away from it. Subsequently, the another vortex system (B) divides into two systems in the same way as the vortex system (A). The larger vortex systems outside the systems beside the cylinder move gradually anticlockwise with increasing the oscillation amplitude. Then the flow field separates into two regions and the small inner vortex systems are isolated in the thin layer beside the cylinder, as shown in Fig. 4 (e). On the other hand, the large vortex systems in the outer flow region move anticlockwise still more and turn into the outer vortex systems, with a direction of circulation such that the flow is away from the cylinder along the axis of oscillation and toward it perpendicular to the axis, as shown by the arrow in Fig. 4 (e) and (f). In this way, the inner vortex systems shrink down at a certain critical value of the oscillation amplitude and four outer vortex systems become conspicuous. When the oscillation amplitude is increased larger than the critical value s_c, the inner vortex systems shrink down still smaller and the outer vortex systems become dominant, as shown in Fig. 4 (f). The process of the transition of the flow pattern around an elliptic cylinder is similar to that around a triangular cylinder but shows its own characteristics.

Figure 5 shows some photographs of the consecutive stages of the flow around an elliptic cylinder when the oscillation amplitude was increased in steps at $r_0\sqrt{\omega/\nu}=5.36$. As will be seen from Fig. 5 (a), the inner vortex system (A) naturally divides into two systems even at small values of oscillation amplitude. Such a flow pattern appears approximately in the range of $5<r_0\sqrt{\omega/\nu}<7$.

The photographs in Fig. 6 show the streaming at $r_0\sqrt{\omega/\nu}=8.36$. The inner vortex systems are small and the outer vortex systems are dominant. Thus, the thickness of the inner vortex systems become smaller with increasing the values of $r_0\sqrt{\omega/\nu}$. On the other hand, the thickness of the inner vortex systems are independent of the values of the oscillation amplitude when it is small, as will be seen from Fig. 6 (a) and (b). Such properties

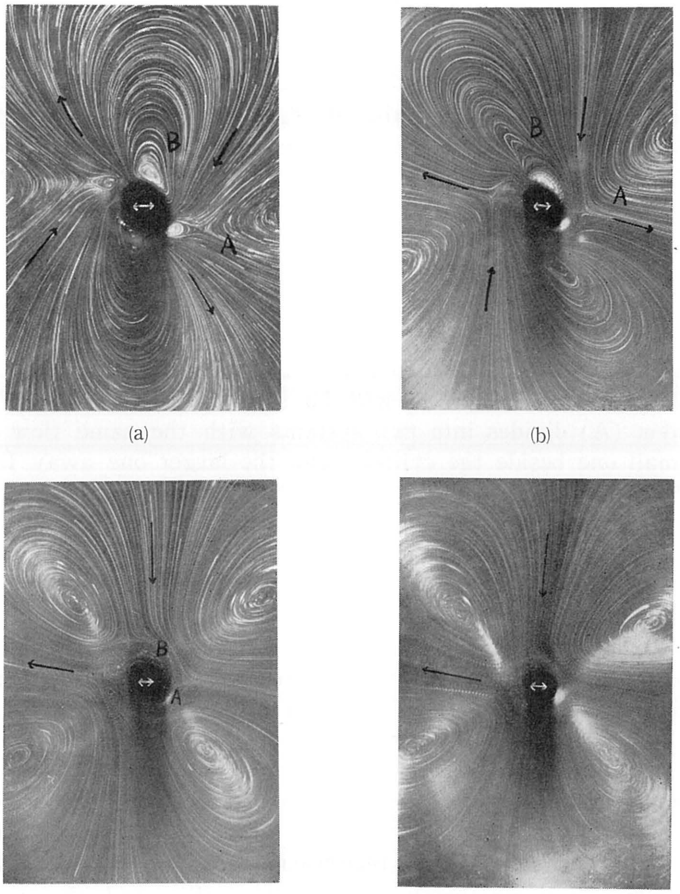

(a) (b) (c) (d)

Fig. 5 Consecutive stages of the flow around an elliptic cylinder when the oscillation amplitude was increased in steps.
$r_0=0.207$ cm, $f=30.0$ Hz, $\nu=0.28$ cm^2/s, $r_0\sqrt{\omega/\nu}=5.36$.
(a) $s/r_0=0.146$, $t_e=60$ s (b) $s/r_0=0.585$, $t_e=30$ s
(c) $s/r_0=0.754$, $t_e=10$ s (d) $s/r_0=0.986$, $t_e=12$ s
Aluminium dust and glass micro-particles were added to serve as tracers.

of the inner vortex systems are common to that of some bodies investigated up to date.

Figure 7 shows the streaming at $r_0\sqrt{\omega/\nu}=12.5$ and $s/r_0=0.0754$. The thickness of the inner vortex systems are considerably small.

Here, quantitative measurements were done on the values of θ_1, θ_2, l_1 and l_2, which are defined as shown in Fig. 8. The angle θ_1 indicates the position of the stagnation point on the cylinder surface of the flow toward the cylinder and θ_2 indicates that of the flow away from the cylinder. The

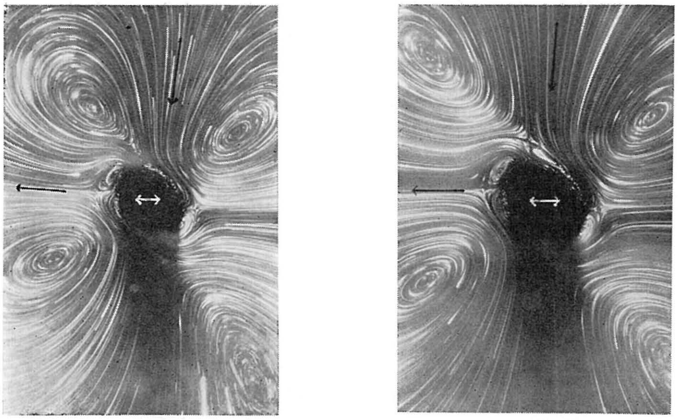

(a) (b)

Fig. 6 Circulatory streaming around an elliptic cylinder at $r_0\sqrt{\omega/\nu}=8.36$.
$r_0=0.207$ cm, $f=50.4$ Hz, $\nu=0.194$ cm^2/s, $r_0\sqrt{\omega/\nu}=8.36$.
(a) $s/r_0=0.0831$, $t_e=60$ s (b) $s/r_0=0.174$, $t_e=30$ s
Aluminium dust method was used.

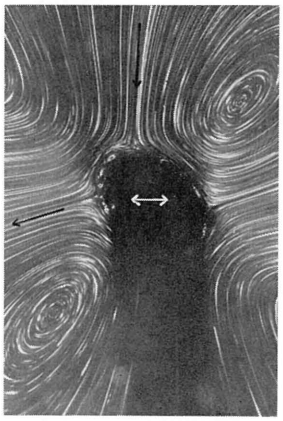

Fig. 7 Circulatory streaming around an elliptic cylinder at $r_0\sqrt{\omega/\nu}=12.5$.
$r_0=0.207$ cm, $f=50.2$ Hz, $s=0.0156$ cm, $\nu=0.087$ cm^2/s, $r_0\sqrt{\omega/\nu}=12.5$, $s/r_0=0.0754$, $t_e=120$ s.
Aluminium dust method was used.

values of l_1 and l_2 indicate the distance between the central axis of the cylinder and the cores of the inner vortex system (A) and (B), respectively. In these measurements the cylinder was stopped optically in the center position of oscillation by using a stroboscope synchronized with the cylinder motion. The values of θ_1 and θ_2 are plotted against s/r_0 in Fig. 9 for each

$r_0\sqrt{\omega/\nu}$. As will be seen from this figure, θ_1 and θ_2 are independent of both $r_0\sqrt{\omega/\nu}$ and s/r_0 within the limits of $r_0\sqrt{\omega/\nu}<9.36$ and $s/r_0<1$. The value of θ_1 is approximately equal to $-5°$ and θ_2 is scattered within the value of 115° to 116°. The values of l_1/r_0 and l_2/r_0 are plotted against s/r_0 in Fig. 10 for each $r_0\sqrt{\omega/\nu}$. This figure indicates that l_1/r_0 and l_2/r_0 are independent of the oscillation amplitude when it is small. In Fig. 11 l_1/r_0 and l_2/r_0, which are independent of the oscillation amplitude, are plotted against

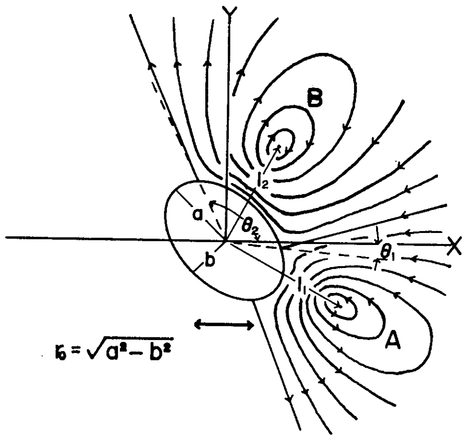

Fig. 8 Definition of the positions of the stagnation points and vortex systems' cores.

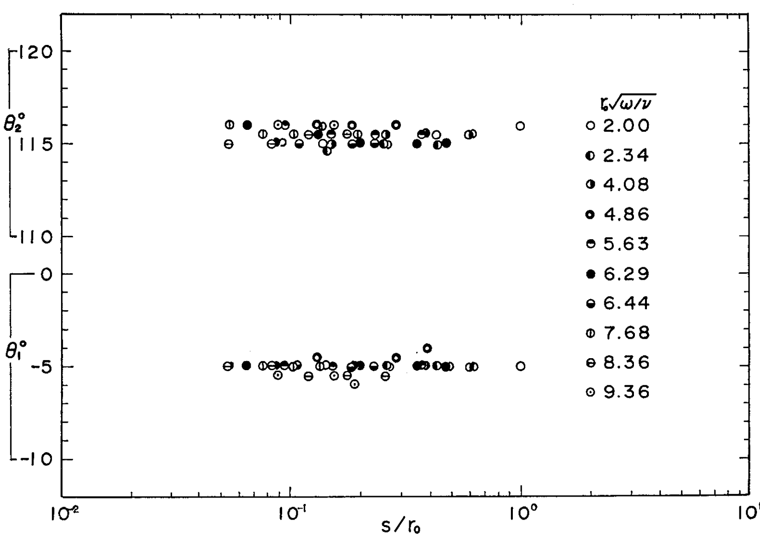

Fig. 9 Positions of the stagnation points on the cylinder surface.

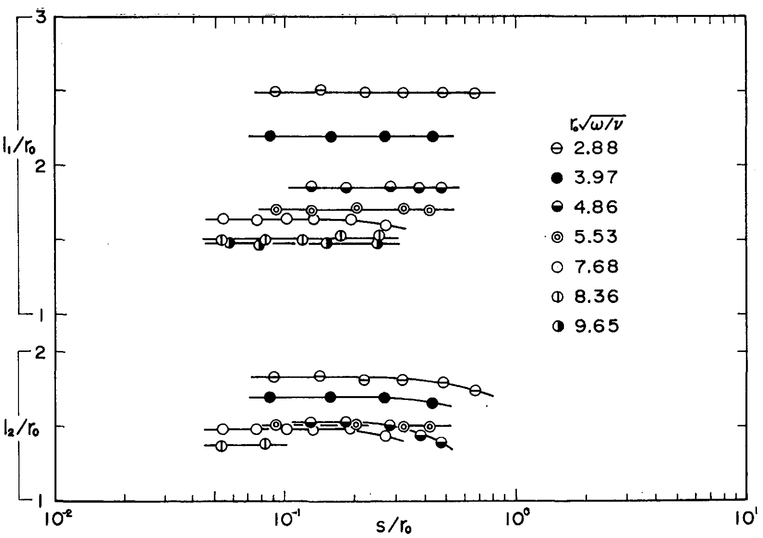

Fig. 10 Distance between the central axis of the cylinder and the core of each inner vortex system.

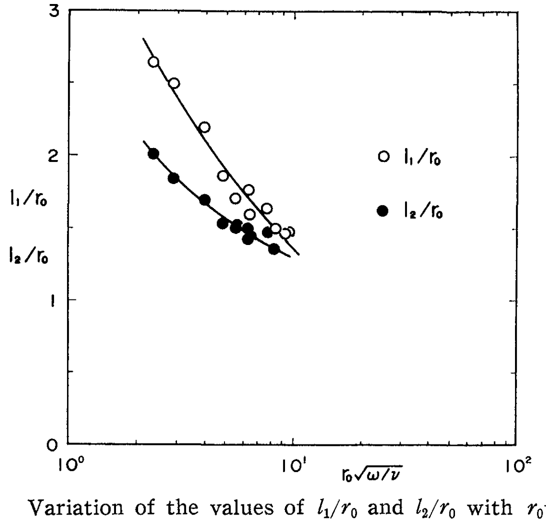

Fig. 11 Variation of the values of l_1/r_0 and l_2/r_0 with $r_0\sqrt{\omega/\nu}$.

$r_0\sqrt{\omega/\nu}$. According as the value of $r_0\sqrt{\omega/\nu}$ is increased, the cores of the inner vortex systems move toward the cylinder. As mentioned above, when the oscillation amplitude is increased to a certain critical value s_c, the inner vortex systems shrink down. The critical value s_c/r_0 at the transition point of the flow pattern is plotted against $r_0\sqrt{\omega/\nu}$ in Fig. 12. From this figure,

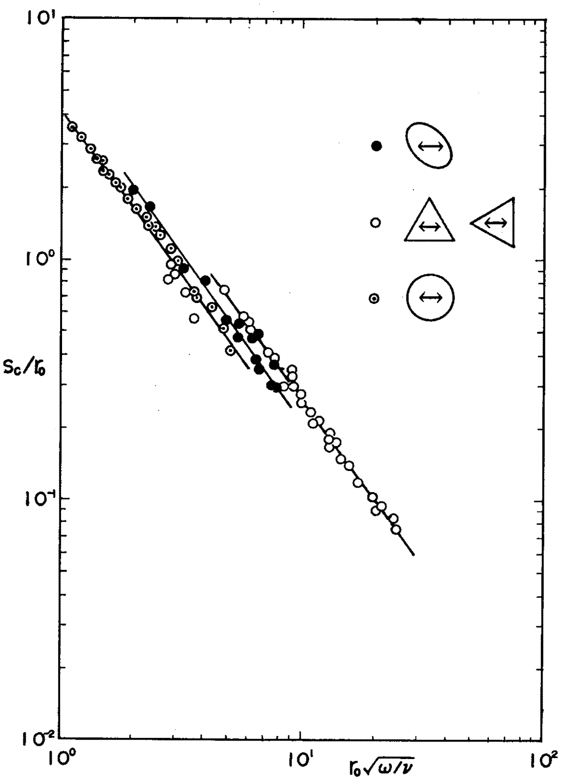

Fig. 12 Relationship between s_c/r_0 and $r_0\sqrt{\omega/\nu}$.

it can be seen that s_c/r_0 is nearly proportional to $(r_0\sqrt{\omega/\nu})^{-1.4}$. In Fig. 12, in addition to the points for the elliptic cylinder, points are included for a circular cylinder and a triangular cylinder. Three straight lines joining points for each body are nearly parallel to each other.

3–2 Case of the minor axis coinciding with the axis of oscillation

In this case, the elliptic cylinder is symmetric with respect to both the axis of oscillation and the axis perpendicular to it. Figure 13 shows some photographs of the flow around the elliptic cylinder for different oscillation amplitude at $r_0\sqrt{\omega/\nu}=4.82$. When the value of $r_0\sqrt{\omega/\nu}$ is small, the inner vortex systems extend broadly. The flow pattern is symmetric with respect to both the axis of oscillation and the axis perpendicular to it. When the oscillation amplitude is increased close to a certain critical value, the flow of the inner vortex systems becomes unstable, as shown in Fig. 13 (c). After that the inner vortex systems shrink down sharply and the outer vortex systems become conspicuous (see Fig. 13 (d)). The process of the transition of the flow pattern in this case is different from that of the case *3–1*, in

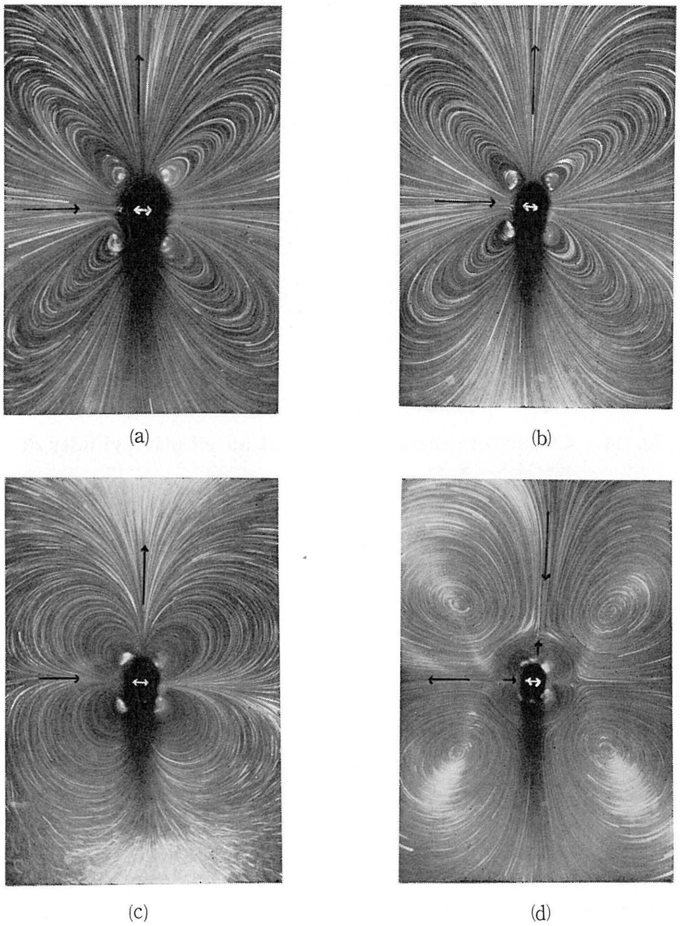

Fig. 13 Consecutive stages of the flow around an elliptic cylinder when the oscillation amplitude was increased in steps.
$r_0=0.206$ cm, $f=60.4$ Hz, $\nu=0.69$ cm^2/s, $r_0\sqrt{\omega/\nu}=4.82$.
(a) $s/r_0=0.166$, $t_e=20$ s (b) $s/r_0=0.254$, $t_e=30$ s
(c) $s/r_0=0.519$, $t_e=30$ s (d) $s/r_0=0.587$, $t_e=20$ s
Glass micro-particles were added to serve as tracers.

which the minor axis of the elliptic cylinder is inclined at an angle 45° with the axis of oscillation. The inner vortex systems don't divide into two systems and shrink down sharply at a certain critical value of the oscillation amplitude. Such process of the transition of the flow is common to that of a circular cylinder or a square cylinder which is symmetric with respect to both the axis of oscillation and the axis perpendicular to it.

The photograph in Fig. 14 shows the flow around the cylinder at $r_0\sqrt{\omega/\nu}=8.34$ and $s/r_0=0.151$. The inner vortex systems are small and the outer

Fig. 14 Circulatory streaming around an elliptic cylinder at $r_0\sqrt{\omega/\nu}=8.34$.
$r_0=0.206$ cm, $f=60.6$ Hz, $s=0.0312$ cm, $\nu=0.232$ cm²/s, $r_0\sqrt{\omega/\nu}=8.34$, $s/r_0=0.151$, $t_e=30$ s.
Glass micro-particles were added to serve as tracers.

vortex systems are dominant.

4 Conclusion

The circulatory streaming generated by an oscillating elliptic cylinder was investigated experimentally.

When the minor axis of the elliptic cylinder is inclined at an angle 45° with the axis of oscillation, the flow pattern of the streaming has symmetry with respect to a turn of 180 degrees around the center axis of the cylinder. The distance between the cores of the inner vortex systems and the center axis of the cylinder is large at small values of $r_0\sqrt{\omega/\nu}$, and becomes smaller with increasing the value of $r_0\sqrt{\omega/\nu}$. The position of the stagnation points on the cylinder surface is independent of both the values of $r_0\sqrt{\omega/\nu}$ and s/r_0. The critical value of s_c/r_0 is nearly proportional to $(r_0\sqrt{\omega/\nu})^{-1.4}$.

On the other hand, when the elliptic cylinder is oscillated in the direction of its minor axis, the flow pattern is symmetric with respect to both the axis of oscillation and the axis perpendicular to it.

Acknowledgements

The author wishes to thank Professor S. Taneda for his valuable advice and encouragement in the course of this work. This work was supported by the Grant-in-Aid for Scientific Research from the Ministry of Education and "The Mitsubishi Foundation".

References

1) Carrière, M. Z., Analyse ultramicroscopique des vibrations aériennes, J. Phys. et radium 6, 10, 1929, p. 198.
2) Andrade, E. N. da C., On the circulations caused by the vibration of air in a tube, Proc. Roy. Soc. L., Ser. A 134, 1931, p. 445.
3) Schlichting, H., Berechnung ebener periodischer Grenzschichtströmungen, Phys. Z., 33, 1932, p. 327.
4) Holtsmark, J., Johnsen, I., Sikkeland, T. and Skavlem, S., Boundary layer flow near a cylindrical obstacle in an oscillating, incompressible fluid, J. Acoust. Soc. Amer., 26, 1954, p. 26.
5) Raney, W. P., Corelli, J. C. and Westervelt, P. J., Acoustical streaming in the vicinity of a cylinder, J. Acoust. Soc. Amer., 26, 1954, p. 1006.
6) Skavlem, S. and Tjötta, S., Steady rotational flow of an incompressible, viscous fluid enclosed between two coaxial cylinders, J. Acoust. Soc. Amer., 27, 1955, p. 26.
7) Stuart, J. T., Double boundary layers in oscillatory viscous flow, J. Fluid Mech., 24, 1966, p. 673.
8) Tatsuno, M., Secondary flow around an oscillating circular cylinder, Bull. Res. Inst. Appl. Mech., Kyushu Univ., 38, 1972, p. 1 [in Japanese].
9) Tatsuno, M., Circulatory streaming around an oscillating circular cylinder at low Reynolds numbers, J. Phys. Soc. Japan, 35, 1973, p. 915.
10) Bertelsen, A., Svardal, A. and Tjötta, S., Nonlinear streaming effects associated with oscillating cylinders, J. Fluid Mech., 59, 1973, p. 493.
11) Lane, C. A., Acoustical streaming in the vicinity of a sphere, J. Acoust. Soc. Amer., 27, 1955, p. 1082.
12) Wang, C. Y., The flow field induced by an oscillating sphere, J. Sound Vib., 2, 1965, p. 257.
13) Riley, N., On a sphere oscillating in a viscous fluid, Quart. J. Mech. and Applied Math., 19, 1966, p. 461.
14) Endoh, K. and Hirano, H., Flow patterns in the vicinity of sphere and circular disk vibrating in liquid, J. Res. Assoc. Powder Tech. Japan, 7, 1970, p. 346 [in Japanese].
15) Tatsuno, M., Circulatory streaming in the vicinity of an oscillating square cylinder, J. Phys. Soc. Japan, 36, 1974, p. 1185.
16) Tatsuno, M., Circulatory streaming in the vicinity of an oscillating triangular cylinder, J. Phys. Soc. Japan, 38, 1975, p. 257.

(Received November 30, 1974; Communicated by S. Taneda)